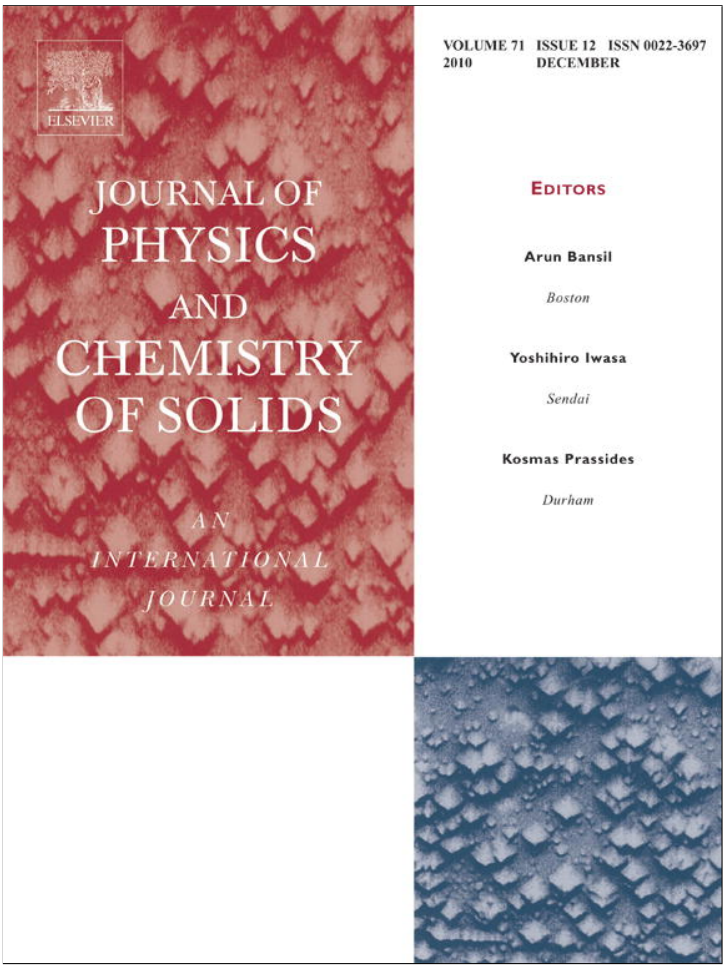

Journal of Physics and Chemistry of Solids 71 (2010) 1634–1638

Contents lists available at ScienceDirect

Journal of Physics and Chemistry of Solids

journal homepage: www.elsevier.com/locate/jpcs

Spatially controlled dissolution of Ag nanoparticles in irradiated SiO_2 sol–gel film

J. Massera [a], A. Martin [b], J. Choi [c], T. Anderson [c], L. Petit [a,*], M. Richardson [c], Y. Obeng [d], K. Richardson [a]

[a] School of Materials Science and Engineering, Clemson University, Clemson, SC 29634, USA
[b] Institut de Chimie de la Matiere Condensee de Bordeaux (ICMCB), CNRS UPR 9048, Av. du Dr. A. Schweitzer, 33608 Pessac Cedex, France
[c] College of Optics, Center for Research and Education in Optics and Lasers (CREOL), University of Central Florida, Orlando, 4000 Central Florida Boulevard, FL 32816, USA
[d] Nkanea Technologies Inc., 6440 Aylworth Drive, Frisco, TX 75035, USA

ARTICLE INFO

Article history:
Received 24 July 2009
Received in revised form
30 November 2009
Accepted 4 September 2010

Keywords:
A. Glasses
A. Optical materials
A. Thin films
A. Optical properties
A. Surface properties

ABSTRACT

In this paper, we report the spatially controlled dissolution of silver nanoparticles in irradiated SiO_2 sol–gel films. The Ag nanoparticles have been formed in the sol–gel solution before the film deposition by adding Triton and ascorbic acid and also after the film deposition using a heat treatment at 700 °C for few minutes or at 550 °C for 6 h in reducing atmosphere. Using a spectrometer, a new view white light interferometer and a micro-thermal analyzer, we demonstrate that the silver nanoparticles can be dissolved using a continuous black ray UV lamp or with a near-infrared (NIR) femtosecond laser, due to a significantly increase in the local temperature. We confirm that the micro-thermal analyzer can be used as a new tool to study the dissolution of metallic nanoparticles in thin film if located at the surface of the films.

1. Introduction

Small clusters of metallic atoms, commonly called nanoparticles (NPs), are one of the most interesting and quickly developing areas of the solid state physics [1]. The study of these systems includes the development and optimization of various techniques to prepare these metallic nanoparticles [2]. The sol–gel route has been found to be an easy technique to form metallic nanoparticles such as Au and Ag in a temperature stable oxide matrix such as SiO_2 and TiO_2 [3,4]. Silver nanoparticle doped glasses have been extensively studied to develop nanomaterials either for functional optical devices, based on ultrafast optical response [5] and third-order nonlinearity [6] or for sensing applications [7].

The effect of heat treatment on the formation of Ag nanoparticles has been studied intensively. Mennig et al. [8] observed an oxidation of the silver colloids to Ag_xO_y during thermal densification of the films accompanied by the disappearance of yellow color of the coatings. Later, using XPS and RBS, Li et al. [9] confirmed the oxidation process during heat treatment. Yliniemi et al. [10] showed that the long term stability and barrier properties of the films could be tailored by low temperature O_2 and H_2 plasma treatment, which, respectively, induces partial calcination of the film followed by an oxide formation and achieves reduction in Ag nanoparticles. Previous works reported the space-selective precipitation of Au and Ag in silicate-based bulk glasses using fs laser and successive annealing [11,12] while Goutaland et al. [13] have shown that small silver NPs can be formed under UV exposure and large NPs can be formed when both the annealing temperature and the UV power density are high enough. This space-selective precipitation of Ag nanoparticles can provide a solution to optoelectronic devices due to the tight control of NPs' size. However, Chen et al. [14] demonstrated that the oxidation of silver atoms is predominant during high temperature annealing and reduces NPs' growth efficiency, which requires tight focusing of the laser beam.

The purpose of our investigation is to demonstrate the feasibility of controlling the space-selective dissolution of metallic nanoparticles in a single glass matrix with micron-meter resolution. In this paper, first we report results on the precipitation of Ag nanoparticles in SiO_2 sol–gel film by adding electrons donor in the sol–gel solution and also by heat treating the film in various environments. We also discuss the effect of a UV or IR exposure followed by a heat treatment on the dissolution of the Ag nanoparticles. The presence of the Ag nanoparticles has been investigated using a relatively new technique developed in our group that consists of measuring the relative heat flow map using a micro-thermal analyzer [15]. The surface profile of the investigated films has been also measured with a microscope profilometer and the film surface roughness variation is discussed as a function of the formation or the dissolution of the Ag nanoparticles.

* Corresponding author.
E-mail address: lpetit@clemson.edu (L. Petit).

0022-3697/$ - see front matter Crown Copyright © 2010 Published by Elsevier Ltd. All rights reserved.
doi:10.1016/j.jpcs.2010.09.002

2. Experimental procedure

2.1. Film deposition

High purity tetraethylorthosilicate (TEOS; 98%, Sigma Aldrich), silver nitrate (99.9%, Alfa-Aesar), absolute ethanol (99.5% , Sigma Aldrich), nitric acid (certified ACS plus, Fisher), L-ascorbic acid (99%, Sigma Aldrich), Triton X-100 (Sigma Aldrich) and deionised water (DIW) have been used in the experiments. Appropriate amount of the Ag precursor has been dissolved in ethanol and mixed to the solution containing the TEOS then few drops of concentrated HNO_3 have been used as catalyst. The molar ratio of matrix precursor/ethanol/water/HNO_3 has been kept at 1/30/1/0.03. The final solution has been sealed in a container and stirred continuously at room temperature for 24 h in a dark environment, to avoid an ambient light-induce oxidation of the Ag precursor. Fifteen layers have been spin coated on a pre-cleaned and dried soda-lime substrate and finally the films have been then annealed at 150 °C in air for 15 h. The uniform thickness of the films over a microscope slide scale has been measured to be 600 ± 100 nm using the Zygo New View White Light Interferometer microscope.

2.2. Light source set-up

The cw 366 nm source used during this study is a black ray lamp with a power of 2×6 W (UVL-56, UVP), with a spectral bandwidth of 330–370 nm (FWHM). The films have been exposed for 24 h using this lamp.

The 800 nm source is a chirped-pulse amplified Ti:Al_2O_3 femtosecond laser system (Spitfire, Spectra Physics) operating at 1 kHz with the pulse duration of ~120 fs. The Gaussian laser output beam has been focused by a $10\times$, 0.25-N.A. microscope objective at the surface of the film sample that has been translated perpendicular to the laser beam by a computer-controlled three-axis translation stage. The laser intensity has been adjusted with a half-wave plate and a polarizing cube beamsplitter placed before the microscope objective. To be able to measure the transmission spectra of the film prior to and after irradiation, the exposed regions consisted of 100 μm-by-100 μm squares made by scanning 50 lines spaced 2 μm apart.

2.3. Optical properties measurement

The transmission spectra of the deposited film have been measured with a dual beam UV–vis–NIR Perkin Elmer Lambda 900 spectrophotometer. The measurements have been performed at room temperature in ambient air.

2.4. Surface profile characterization

The film surface topography has been studied with $5\times$ and $20\times$ objectives on a Zygo New View 6300 white light interferometer microscope (Zygo Corporation, Middlefield, CT, USA). This tool has the capability to characterize and quantify surface roughness, step heights and other topographical features. The filter used has been "High Pass" and the filter type "FFT Fixed". No geometry has been removed.

2.5. Localized thermal conductivity/relative heat flow measurements

Local relative heat flow values on films deposited have been determined using a micro-thermal analyzer TA 2990 from TA Instruments as explained in [15]. Depicted schematically in Fig. 1, the instrument combines atomic force microscopy (AFM) with thermal characterization capability by replacing the standard probe in the AFM with a heat resistive wire probe; this modification allows thermal analysis for both the detection of phase transitions and thermal imaging for thermal conductivity determination via the measurement of heat flow. For each scan, both the topographic and the heat flow images are recorded. As heat can flow from the probe tip both to the sample and to the silver probe supports and surrounding air, there is a background heat flow, which is unrelated to the sample. It is therefore important to measure this background heat loss by placing the probe at a set distance above the sample surface (200 μm) and repeating the thermal scan. The relative heat flow between the probe and sample (Q) can be estimated using the equation

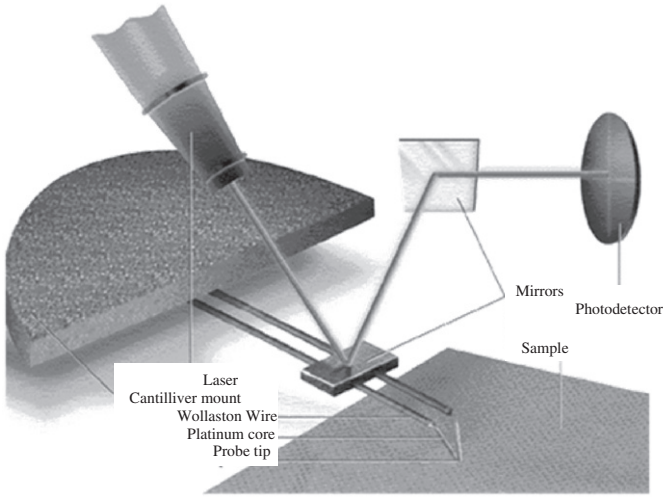

Fig. 1. Diagram of probe configuration for micro-thermal analysis using the μTA 2990 (image supplied by TA Instruments).

$$\frac{P_c - P_{nc}}{P_c} = Q \tag{1}$$

where P_c and P_{nc} are the probe power (mW) for contact (Fig. 2a) and non-contact measurements (Fig. 2b), respectively.

The mean relative heat flow has been taken from the histogram of the heat flow deviation data (Fig. 2d) and the accuracy of the mean relative heat flow has been estimated at ± 0.01. A temperature controlled stage at 27 °C and a probe temperature of 127 °C have been utilized in order to prevent variations caused by changes in ambient thermal conditions. Surface scans have been performed on three randomly chosen 50×50 μm^2 areas, followed by an identical reference scan in air immediately at a constant height of ~200 μm above the sample surface.

3. Results and discussion

Ag doped SiO_2 sol–gel films have been prepared by spin coating a sol–gel solution doped with silver nitrate used as the precursor for the Ag nanoparticles on a soda-lime substrate. Fig. 3a exhibits the transmission spectrum of the film after annealing. One can notice the absence of periodic variations in the transmission value as a function of wavelength caused by the back and front surface reflections. This is probably due to the small thickness of the films and to the low index contrast between lightly doped films and the substrate. Indeed, it is very well known that (i) the upper and lower interference envelopes are dependent on the refractive index and (ii) the distance between the fringes depend on both the refractive index and the thickness of the films [16]. No absorption band related to the presence of

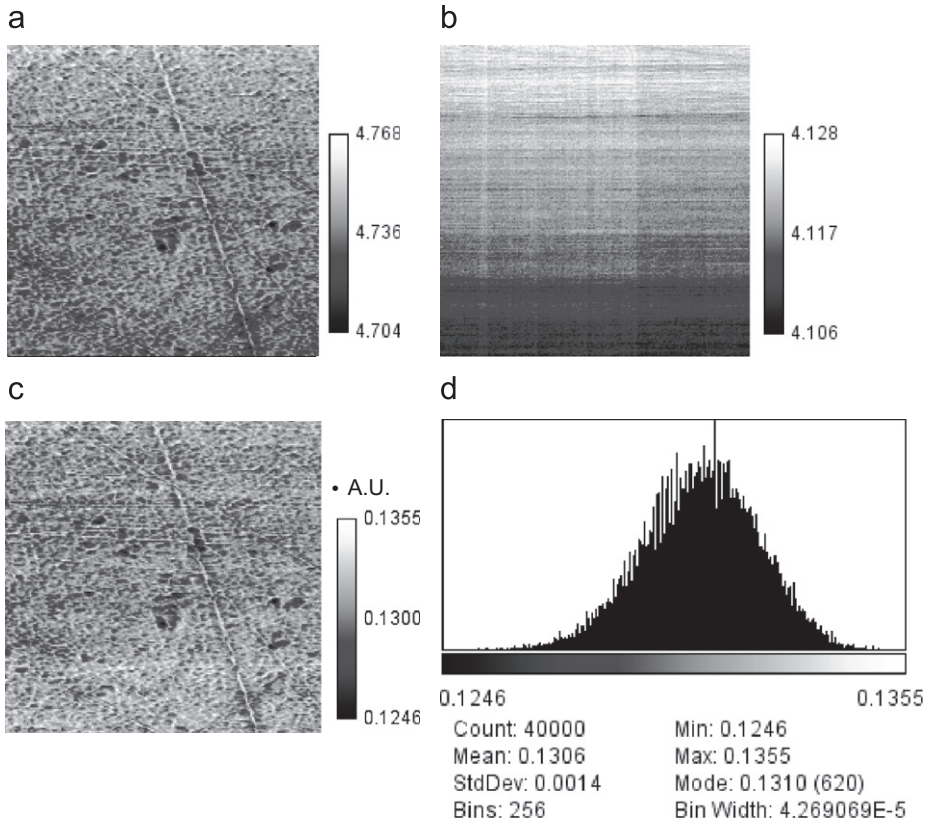

Fig. 2. Sample of image processing procedure: (a) two dimensional contact scan (P_{nc}), (b) non-contact scan (P_c), (c) calculated power deviation (Q_s) and (d) histogram of power deviation (mW) values as a function of pixel count.

Ag nanoparticles can be seen in the spectrum, showing that the silver nitrate can be completely dispersed in the sol–gel solution. We investigated various techniques to process Ag nanoparticles in the SiO_2 sol–gel thin films by precipitating the Ag nanoparticles in the solution or in the annealed film. Solutions have been also prepared with addition of a few drops of Triton X-100, a poly(oxyethylene)isooctyl phenyl ether medium and by substituting the drops of pure water with drops of a solution of 963 mg L-ascorbic acid dissolved in 10 mL of deionised water. Fig. 3a exhibits the transmission spectrum of the Ag doped film deposited from a solution prepared with ascorbic acid and Triton X-100. The spectrum exhibits an absorption band centered in the range 420–430 nm, which can be attributed to the surface plasmon resonance of Ag nanoparticles in agreement with [17]. In agreement with [18], the band can be associated with $(Ag^0)_n$, silver crystallites, where n is the number of silver atoms forming the crystallite. It is interesting to point out the absence of absorption band at 305 and 350 nm, which have been associated with Ag^+ ions and Ag^0 (elemental Ag atoms), respectively, as reported by Ahmed and Abdallah [18]. In agreement with [19,20], the L-ascorbic acid, which acts as an electron donor, is expected to facilitate the reduction of silver ions in metallic silver while the Triton X-100 is expected to form micelles/mesoporous structures that template or confine the reactants into pores, thus providing the driving force for the aggregation of nanoparticles to small aggregates. This idea is further supported by our observations that when sol–gel solutions were prepared with Triton X-100 or L-ascorbic acid separately, no Ag nanoparticles could be formed in the annealed films. The approximate size of Ag nanoparticles can be calculated from the following formula [21]:

$$R = \frac{V_f \lambda_p^2}{2\Pi C \Delta\lambda}$$

where V_f, 1.39×10^8 cm/s, is the Fermi velocity of the electrons in bulk silver, C the speed of light, $\Delta\lambda$ the full-width at half-maximum of the absorption band and λ_p the peak position of the surface plasmon resonance absorption characteristic wavelength at which it occurs.

Based on the formula and on the work reported by Zeng et al. [22], the average radius of the Ag nanoparticles has been estimated to be ~5 nm. In order to form nanoparticles in the film after annealing, the Ag doped films have been heat treated at 700 °C for 2 min in air as suggested by Jeon et al. [23]. The film's color changed from colorless to yellowish. Fig. 3b shows the transmission spectra of the film prior to and after the heat treatment. The transmission spectrum of the film after heat treatment exhibits a band center at ~410 nm confirming the precipitation of Ag nanoparticles in the film probably due to the reduction of Ag^+ to Ag^0. It is interesting to point out that the band is not symmetric and is probably formed by 2 overlapping bands at ~410 and ~425 nm. As the resonance peak grows, sharpens and exhibits redshift with increase in size of nanoparticles [22], it is possible to think that the presence of the two absorption bands at ~410 and ~425 nm reveals the formation of Ag nanoparticles with various diameters. The investigated films were found temporally stable as they did not show any changes in the optical spectra after being exposed to the laboratory ambience for a few days.

The other very well-known technique for forming nanoparticles in sol–gel thin films involves heat treatment of the doped films in a reducing atmosphere, such as 5% H_2 in Ar [8,10,23]. The as-deposited films were heat treated for 6 h at 550 °C in H_2 atmosphere. As observed for the film heat treated at 700 °C, the color of the film changed from colorless to yellowish after the heat treatment. The transmission spectrum of the heat treated film is presented in Fig. 3c and exhibits an absorption band at 410 nm confirming the

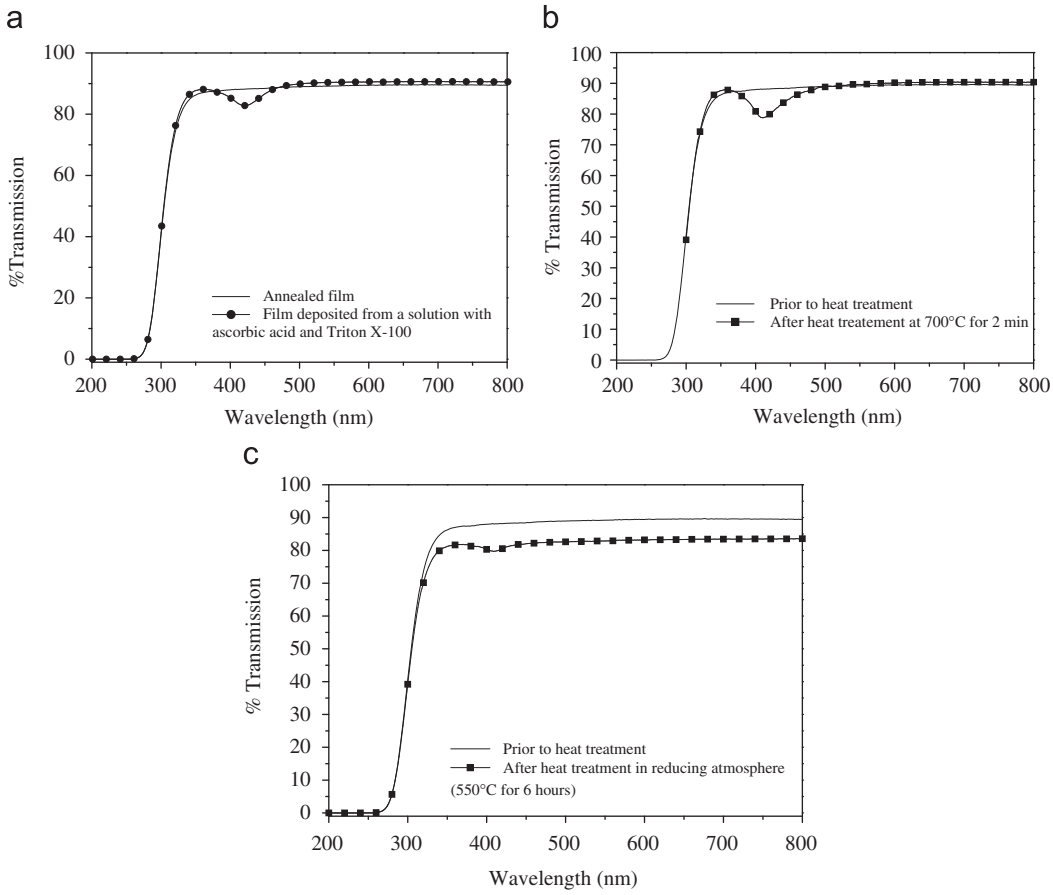

Fig. 3. Transmission spectra of annealed Ag doped films and films deposited from a solution containing Triton X-100 and ascorbic acid (a), after heat treatment at 700 °C for 2 min (b) and at 550 °C for 6 h in reducing atmosphere (c).

formation of Ag nanoparticles as expected by the change in the film color from colorless to yellowish after the heat treatment [8,10,23]. However, one may notice that the amplitude of the absorption band at 410 nm is smaller than that in Fig. 3a and b.

We have focused our effort on the use of light exposure to spatially control the dissolution of the Ag nanoparticles on a micrometer resolution. Thus, the Ag containing films processed using ascorbic acid and Triton X-100 were irradiated for 24 h with a continuous (cw) UV lamp with an intensity of 4.8 mW/cm^2 and also with a NIR fs laser with an intensity of 1.4 and 1.6 TW/cm^2. No significant changes in the coloration of the film were observed after cw irradiation. Due to the small size of the irradiated area (100 μm × 100 μm) using the pulsed laser, it was not possible to observe any changes in the film coloration after the laser irradiation. To confirm the changes in the Ag nanoparticle size and/or content in the film, the transmission spectrum of the irradiated areas was measured after irradiation. As seen in Fig. 4, the amplitude of absorption bands associated with the Ag nanoparticles decreases slightly after the cw light exposure in agreement with the absence of dramatic changes in the film color and decreases more dramatically after exposure with the NIR fs laser confirming that it is possible to dissolve the Ag nanoparticles using continuous black ray UV lamp or with a near-infrared (NIR) femtosecond. The progressive decrease in the absorption band amplitude can be attributed to changes in the particles size: from particles to cluster and from cluster to ion leading to dissolution of Ag nanoparticles, in agreement with [24–26]. Stalmashonak et al. [26] found that irradiating samples preheated to 150–200 °C results in dissolution of Ag nanoparticles and complete bleaching of SP resonance. A similar effect was observed for irradiation at room temperature at higher repetition

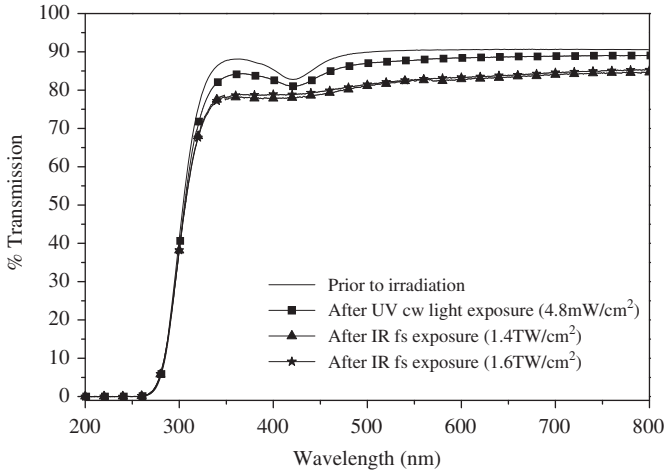

Fig. 4. Transmission spectra of Ag nanoparticles containing films before and after UV and IR irradiation.

rate, which can be explained by heat accumulation in the focal volume. The larger variation in the transmission spectrum after pulsed laser irradiation might be related to the larger intensity of the laser as compared to the cw exposure. It is expected that the ultrahigh intensity of the fs laser promotes more than two-photon absorption resulting in a significant increase in the local temperature at the focus point of the laser, driving the conversion of nanoparticles into ions or individual atoms. Indeed, in agreement with previous study [15], the temperature of the film surface during

the cw and fs light exposure is expected to increase to <300 and >1000 °C, respectively.

As performed on chalcogenide glasses [27], squares were written at the surface of the films by translation of the bulk material transversally with respect to the focused laser beam by using a three-dimensional motorized translation stage. As the laser intensity can be adjusted with a variable metallic neutral-density filter placed before the microscope objective, we will be able to control the laser power and thus the dissolution of the Ag nanoparticles. As seen in Fig. 4, we are able to dissolve Ag nanoparticles in a $100\,\mu m \times 100\,\mu m$ area using a pulsed laser. By placing the film on the computer-controlled three-axis translation stage and using a microscope objective, we expect to be able to space selectively dissolve Ag nanoparticles by focusing the laser beam at the surface of the film to dissolve the Ag nanoparticles in spots (or lines) with a diameter as small as 5–10 μm.

The surface morphology of the investigated films has been investigated using a Zygo New View 6300 white light interferometer microscope. The Ag nanoparticles free films exhibit a surface morphology with a root-mean-squared (RMS) roughness of $\sim 40 \pm 5$ nm whereas the surface roughness of the Ag nanoparticles containing films increases to $\sim 100 \pm 5$ nm as expected. The surface roughness of the Ag containing film measured after laser irradiation was found to decrease to $\sim 15 \pm 5$ nm probably due to the dissolution of the Ag nanoparticles. The relative heat flow of the film surface has been measured using the micro-thermal analyzer, TA 2990 from TA instruments. The relative mean heat flow of the Ag nanoparticles free films has been measured at 0.18 ± 0.01. The Ag nanoparticles containing films exhibit a heat flow at 0.22 ± 0.01. A similar increase in the heat flow of Cu doped thin film was measured when Cu nanoparticles were precipitated in the film [15], confirming that the micro-thermal analyzer can be used to verify the presence of metallic nanoparticles in sol–gel film. However, it is interesting to mention that the relative mean heat flow of the Ag nanoparticles containing films prepared with Triton X-100 and ascorbic acid was measured at $\sim 0.19 \pm 0.01$ nm, which, in the accuracy of the measurement, is similar to the relative mean heat flow of the Ag nanoparticle free films. The absence of the mean relative heat flow increase even in the presence of Ag nanoparticles in the film might indicate that the Ag nanoparticles are probably not located at the surface of the films in agreement with our previous work [15].

4. Conclusion

In this paper, different techniques have been used to spatially control the precipitation and the dissolution of silver nanoparticles in sol–gel films. We explain that ascorbic acid and Triton can be used to form silver nanoparticles in the sol–gel solution while a heat treatment for 2 min at 700 °C in air or at 550 °C for 6 h in a reducing atmosphere can form silver nanoparticles in silica sol–gel films. We confirm that these silver nanoparticles can be dissolved locally using UV and near-infrared light exposure principally due to heat. Finally, we show that the formation of silver nanoparticles leads not only to an increase in the film surface roughness but also to an increase of the relative mean heat flow, measured using a micro-thermal analyzer. We confirm that this new technique developed in our group can only detect nanoparticles if located at the surface of the films.

References

[1] W.P. Halperin, Rev. Mod. Phys. 58 (1986) 533.
[2] J.A.A.J. Perenboom, P. Wyder, F. Meier, Phys. Rep. 78 (1981) 173.
[3] G. Mitrikas, C.C. Trapalis, G. Kordas, J. Non-Cryst. Solids 286 (2001) 41.
[4] U. Schubert, New J. Chem. 18 (1994) 1049.
[5] R. Philipp, G.R. Kumar, N. Sandhyarani, T. Pradeep, Phys. Rev. B 62 (2000) 13160.
[6] K. Uchida, S. Kaneko, S. Omi, C. Hata, H. Tanji, Y. Asahara, A.J. Ikushima, T. Tokizaki, A. Nakamura, J. Opt. Soc. Am. B 11 (1994) 1236.
[7] H. Jia, J. Zeng, W. Song, J. An, B. Zhao, Thin Solid Films 496 (2006)) 281.
[8] M. Mennig, M. Schmidt, H. Schmidt, J. Sol–Gel Technol. 8 (1997) 1035.
[9] W. Li, S. Seal, E. Megan, J. Ramsdell, K. Scammon, G. Lelong, L. Lachal, K. Richardson, J. Appl. Phys. 93 (12) (2003) 9553.
[10] K. Yliniemi, P. Ebbinghaus, P. Keil, K. Kontturi, G. Grundmeier, Surf. Coat. Technol. 201 (2007) 7865.
[11] X. Hu, Q. Zhao, X. Jiang, C. Zhu, J. Qiu, Solid State Commun. 138 (2006)) 43.
[12] N.H. Ma, H.L. Ma, M.J. Zhong, J.Y. Yang, Y. Dai, G. Ye, Z.Y. Yue, G.H. Ma, J.R. Qiu, Mater. Lett. 63 (2009) 151–153.
[13] F. Goutaland, E. Marin, J.Y. Michalon, A. Boukenter, Appl. Phys. Lett. 94 (2009) 181108.
[14] S. Chen, T. Akai, K. Kadono, T. Yasawa, Chem. Commun. 20 (2001) 2090.
[15] J. Massera, J. Choi, L. Petit, M. Richardson, Y. Obeng, K. Richardson, Mater. Res. Bull. 43 (2008) 3130–3139.
[16] R. Swanepoel, J. Phys. E: Sci. Instrum. 16 (1983) 1214–1222.
[17] M.A. Garcia, S.E. Paje, J. Llopis, M.A. Villegas, J.M. Fernandez Navarro, J. Phys. D 32 (1999) 975.
[18] A. Ahmed, E. Abdallah, J. Am. Ceram. Soc. 78 (10) (1995) 2777.
[19] L. Suber, I. Sondi, E. Matijevic, D.V. Goia, J. Colloid Interface Sci. 288 (2005) 489.
[20] A. Pal, T. Pal, J. Raman Spectrosc. 30 (1999) 199.
[21] G. Mie, Ann Phys 25 (1908) 377.
[22] H. Zeng, J. Qiu, X. Jiang, C. Zhu, F. Ga, J. Cryst. Growth 262 (2004) 255–258.
[23] H.-J. Jeon, S.-C. Yi, S.-G. Oh, Biomaterials 24 (2003) 4921.
[24] Q.-Z. Zhao, J.-R. Qiu, X.-W. Jiang, C.-J. Zhao, C.-S. Zhu, Opt. Express 12 (17) (2004) 4035.
[25] S. Shibata, K. Miyajima, Y. Kimura, T. Yano, J. Sol–Gel Sci. Technol. 31 (2004) 123.
[26] A. Stalmashonak, A. Unal, H. Graener, G. Seifert, J. Phys. Chem. C 113 (2009) 12028–12032.
[27] L. Petit, N. Carlie, T. Anderson, M. Couzi, J. Choi, M. Richardson, K. Richardson, Opt. Mater. 29 (2007) 1075–1083.